Effect of substituted Mn on optical properties of indium oxide and zinc oxide

M. M. Amiri[1], F. Amiri[2]*, F. Foroutan[2], H. Asghar Rahnamaye Aliabad[3]

[1]Department of Physics, Science Faculty, University of Zabol, Zabol, Iran;
[2]Department of Physics, Islamic Azad University of Mashhad, Mashhad, Iran;,
[3]Department of Physics, Hakim Sabzevari University, Sabzevar, Iran;

Improving the optical properties of materials in the industry is of particular importance. In this paper, we investigated the effect of manganese succession on indium oxide and zinc oxide. Using first-principles based on the density functional theory, the relationship between band structures and optical properties is examined. The full potential linearized augmented plane wave (FP-LAPW) method is employed accompanied by the generalized gradient approximation (GGA). Optical spectra calculations are done for the energy range 0–40 eV. The obtained results indicate that the band structure decreases for In_2O_3 and increases for ZnO by adding Mn. The optical results reveal that the static Dielectric function increases for In_2O_3 and decreases for ZnO due to the Mn dopant. It was observed that the static refractive index for doped indium oxide increased and for doped zinc oxide decreased.
Keywords: Indium Oxide, Zinc Oxide, Band structure, Density Functional Theory

INTRODUCTION

Metallic oxides are a class of materials indicating one of the greatest range of characteristics including superconducting, ferroelectric, ferromagnetic [1], multiferroic, magneto-resistive, dielectric, or conducting. Of special interest is the transparent conducting oxides (TCOs) and amorphous semiconducting oxides (ASOs).

Transparent conducting oxides (TCOs) like In_2O_3, SnO_2, ZnO and CdO are n-type wide band-gap semiconductor materials. Thin films of these elements have been provided by various methods which are fundamental components in optoelectronic devices, like transparent electrodes in panel displays, in thin-film transistors and in infrared reflectors[2-4]. They show high transmittance in the visible and near-infrared domain. The electrical and optical properties of these materials can be changed by introducing impurities. The doped TCO films characteristics are very sensitive to the type of impurities. To know how the structure and properties are affected when the composition changes, it is interesting to investigate the alloys of these elements[5].

ZnO is the other well-known TCO, especially for photovoltaic applications. Zinc oxide can be used as direct wide-band gap semiconductor with band gap energy of 3.3 eV at 300K which is widely employed for production of green, blue-ultraviolet, and white light-emitting devices. ZnO crystallizes in the wurtzize, zinc blende, and rocksalt structures, while the stable phase is wurtzite [8] with regard to thermodynamics. Thermodynamically, the zinc blende ZnO structure is metastable; it can be achieved only by hetero-epitaxial growth on cubic symmetry substrates, such as ZnS GaAs/ZnS[9].

In this study, the impact of Mn dopant on optical properties of In_2O_3 in the cubic bixbyite structure (Fig. 1(a)) and ZnO in phase zinc blende is compared (Fig. 1(b)). From two perspective, the transition metal impurities are of special interest. One manages acceptor-like doping with regards to electronic characteristics. The other manages magnetic characteristics when the concentration of transition element is proportionately high yet inside the dilute limit so as not to change the fundamental basic nature of the ZnO matrix[9].

METHOD OF CALCULATION

The computations are accomplished by means of a self- consistent plan by solving the Kohn- Sham equations using the Full- Potentiol Linearized Augmented Plane Wave (FP-LAPW) method in the structure of density functional theory with the generalized gradient approximation (GGA) method [10,11] using WIEN2k codes [12,13].

The computation is carried out with 1000 k-points for calculating optical part and $Rk_{max}=7$ (R is the smallest muffin- tin radius and k_{max} is the cut- off for the plane wave) for the convergence factor for which the computations stabilize and converge regarding the desired charge. The value of $G_{max}=12$ (the magnitude of largest vector in charge density Fourier expansion or the plane wave cut-off), and the muffin- tin radii for In, Zn, O and Mn are $R_{MT}(In)=2.0$ au , $R_{MT}(Zn)=1.9$ au , $R_{MT}(O)=1.6$ au and $R_{MT}(Mn)= 1.8$ au, respectively. The iteration is stopped when the charge contrast is under 0.0001e

---

* To whom all correspondence should be sent:
E-mail: f.amiri153@gmail.com

between steps as convergence criterion. The cut-off energy, which defines the separation of the valence and core states, is selected to be -6 Ry.

Firstly, the calculations are done by utilizing the experimental data for the lattice constants. Then, the theoretical lattice constants are calculated with optimizing the total energy of crystal to the volume. The final calculation is done with the theoretical lattice constant and relaxed structure for In_2O_3, $In_{1.5}Mn_{0.5}O_3$, ZnO and $Zn_{0.875}Mn_{0.125}O$. The results are indicated in Table 1 which are in agreement with the other results.
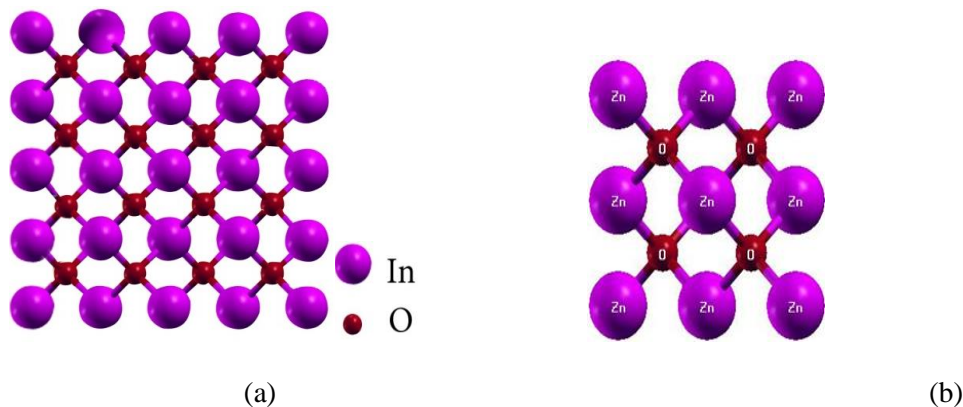

(a)   (b)

Fig. 1. The unit cells of (a) In_2O_3 (b) ZnO

Table 1. Calculated lattice constants for In_2O_3 and ZnO in pure and doped with Mn states.

Compound	This work(Å)	Others(Exp., Å)
In_2O_3	10.059	10.117[13]
ZnO	4.623	4.655[14]

RESULTS AND DISCUSSION
Band structure

Using the GGA approach, the values of the band gaps of pure In_2O_3 and ZnO are computed and alloyed $In_{1.5}Mn_{0.5}O_3$, and $Zn_{0.875}Mn_{0.125}O$ from the band structure, respectively, as shown in Figs. 2 and 3 . The energy scale in all figures is in eV and the Fermi level is set to zero on the energy scale. The valence bands are separated by 1.4 eV and 0.75 eV for undoped In_2O_3 and ZnO energy gap directly from the conduction band states at Γ point. The experimental value of In_2O_3 direct band gap is around 3.6 eV at Γ point[14, 15] and experimental results of ZnO indicate a direct band gap around 3.3eV[16]. These values of band gaps are smaller than the experimental results due to the outstanding gap problem, whereby the DFT undervalues the band gaps. The band gap results for In_2O_3 and ZnO are in accord with the theoretical previous studies such as the reported studies in Ref[17,18].

The obtained band structure of $In_{1.5}Mn_{0.5}O_3$ is presented in Fig.2.b. In this case, energy gap is indirect (at Γ point)1.2 eV.

According to the results of band structure for $Zn_{0.875}Mn_{0.125}O$, the band gap energy increases by adding Mn which is 0.9 eV.

OPTICAL PROPERTIES
Dielectric function

The study focuses on the optical properties of In_2O_3 and ZnO in the pure and doped with Mn states.

The frequency- dependent dielectric function $\varepsilon(\omega)$ is calculated; it describes the characteristics of the linear response of the system to electromagnetic radiation and really controls the spreading behavior of radiation in a medium. $\varepsilon(\omega)$ is associated with the interaction of photons with electrons.

However, the random phase approximation (RPA) approach is used for computing the imaginary part of dielectric function for pure In_2O_3, ZnO and doped with Mn. The real part of dielectric function is computed by utilizing the Kramers- Kronig transformation.

The real and imaginary parts of the frequency dependent dielectric function for In_2O_3 and ZnO in pure state and doped with Mn state are indicated in Figures 4 and 5.

The static dielectric permittivity tensor, $\varepsilon_{\alpha\beta}(0)$, of a nonpolar material includes electronic (high-frequency) and ionic commitment; its square is equivalent to refractive index. Table 2 indicates the high- frequency dielectric constant, $\varepsilon(\infty)$, of In_2O_3, $In_{1.5}Mn_{0.5}O_3$, ZnO and $Zn_{0.875}Mn_{0.125}O$.

The obtained results demonstrate that refraction index increases by adding Mn to Indium Oxide while it decreases by adding dopant Mn to Zinc Oxide.
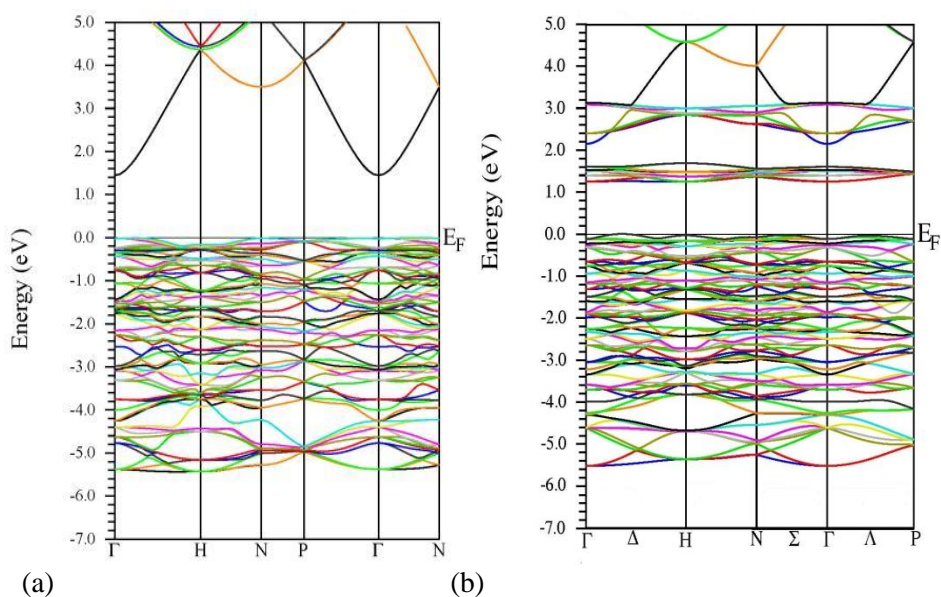
(a)   (b)

Fig. 2. Band structure of (a) pure In_2O_3 (b) of $In_{1.5}Mn_{0.5}O_3$.
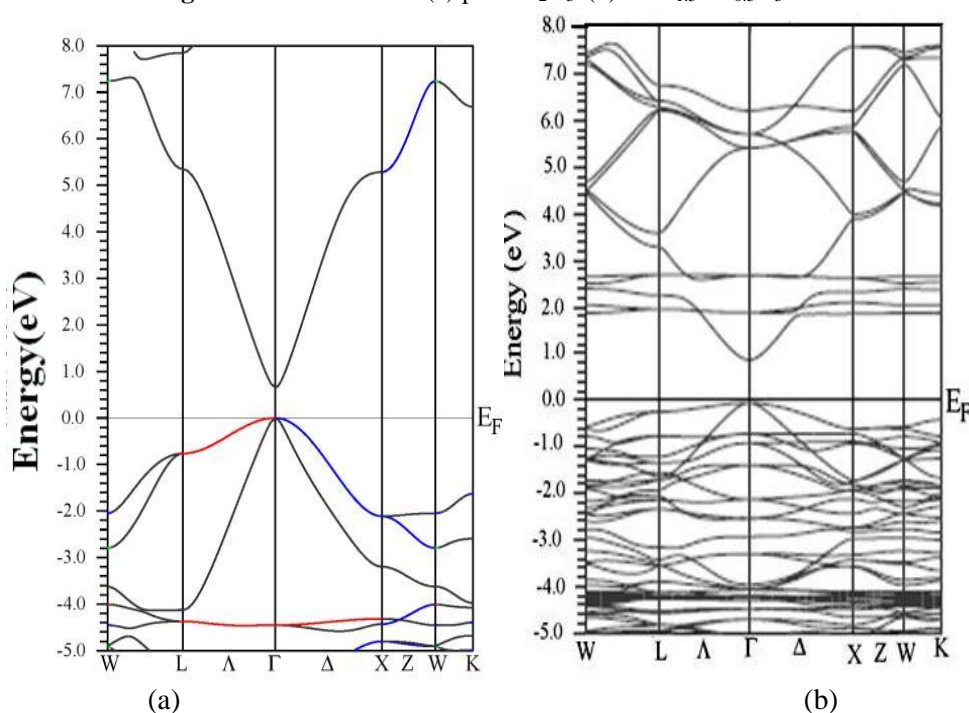

(a)   (b)

Fig. 3. Band structure of (a) pure ZnO **(b)** $Zn_{0.875}Mn_{0.125}O$.

Table 2. High-frequency dielectric constants, ε (∞), of In_2O_3 and ZnO in pure and alloyed with Mn.

Method	In_2O_3	$In_{1.5}Mn_{0.5}O_3$	ZnO	$Zn_{0.875}Mn_{0.125}O$
This work	4.40	4.98	4.88	3.93
Theoretical	4.54[19]	-	3.78[21]	-
Experimental	3.62[20]	-	-	-

In Figure 5, the calculated $Im\varepsilon(\omega)$ shows that the first peak is at $E_0 = 1.46$ eV according to the band structure which is due to the fundamental gap. This peak is related to the interband transition from the valence to the conduction band states at the Γ-point. To simplify the analysis of other optical transition spectra, the labels E_0, E_1 and E_2 have been used. Subscript 0, 1, 2 refer to the transitions along the Γ direction, Γ–N direction, and Γ–P of k-space, respectively.

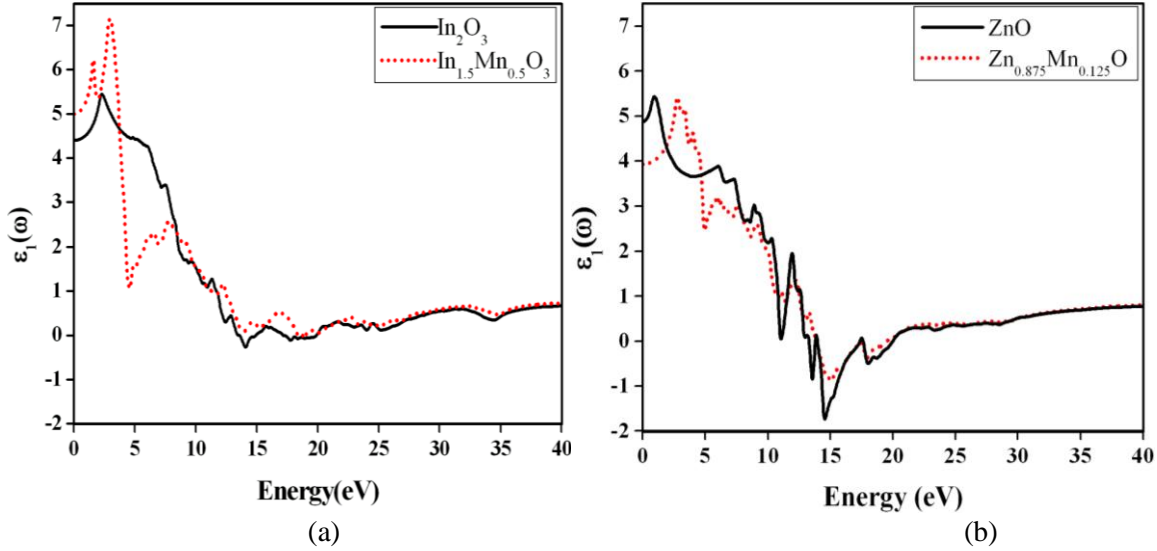In figure 5(b), the compounds E_0, E_1 and E_2 are related to transitions along the Γ–Γ, Γ–L and Γ–X direction.

Fig. 4. Real part of the dielectric function for: (a) In_2O_3 and $In_{1.5}Mn_{0.5}O_3$ (b) ZnO and $Zn_{0.875}Mn_{0.125}O$.
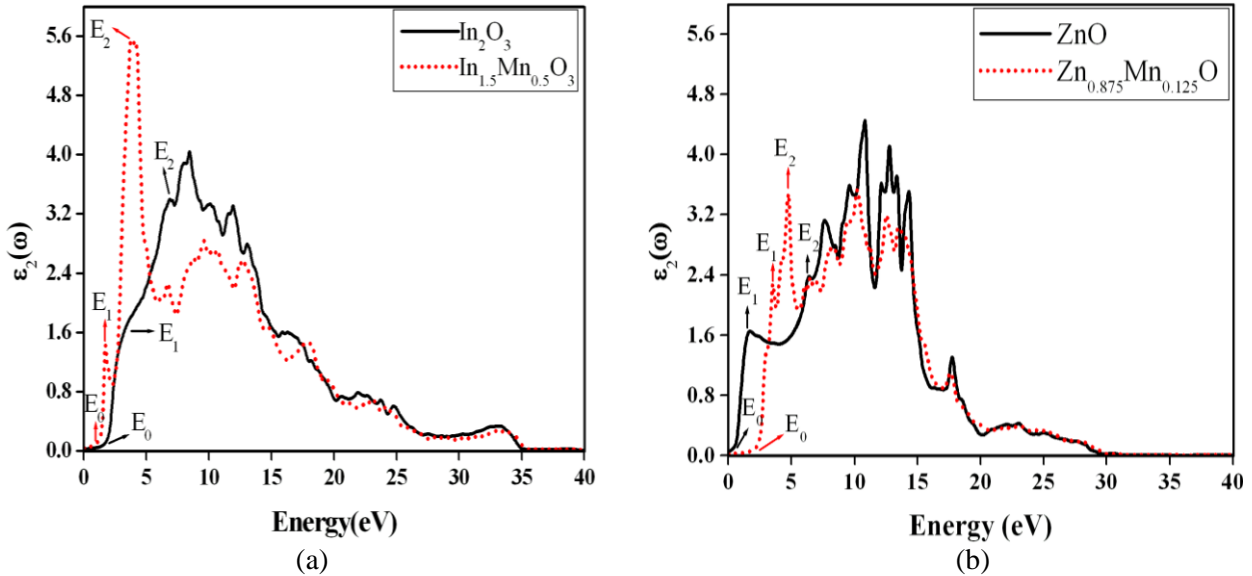

Fig. 5. Imaginary part of the dielectric function for: (a) In_2O_3 and $In_{1.5}Mn_{0.5}O_3$ (b) ZnO and $Zn_{0.875}Mn_{0.125}O$.

Electron energy loss spectroscopy (EELS)

EELS is a valuable tool to examine the different aspects of materials[19- 22] . The advantage of EELS is that it covers the overall energy range including non-scattered and elastically scattered electrons (zero loss), electrons that arouse an atom's outer shell (valence loss) or valence interband transitions. Likewise, the fast electrons arouse the inner shell electrons (core loss) or induce core level excitation of near edge structure (ELNES) and XANES. Regarding interband transitions, this comprises mainly of plasmon excitations. In a direct manner, the probability of scattering for volume losses is associated with the energy loss function. Then, the EEL spectrum can be calculated from the following equations [23]:

$$\varepsilon_{\alpha\beta}(\omega) = \varepsilon_1 + i\varepsilon_2$$

$$EELSpectrum = Im\left[\frac{-1}{\varepsilon_{\alpha\beta}(\omega)}\right] = \frac{\varepsilon_2}{\varepsilon_1^2 + \varepsilon_2^2}$$

Figs. 6 indicates the plot of energy loss function for In_2O_3 and ZnO in pure and alloyed states in the 0–40 eV energy range. The energy of the main maximum of $Im\left[-\varepsilon^{-1}(E)\right]$ is assigned to the energy of volume plasmon $\hbar\omega_P$. The obtained values of $\hbar\omega_P$ are provided in Table 3.

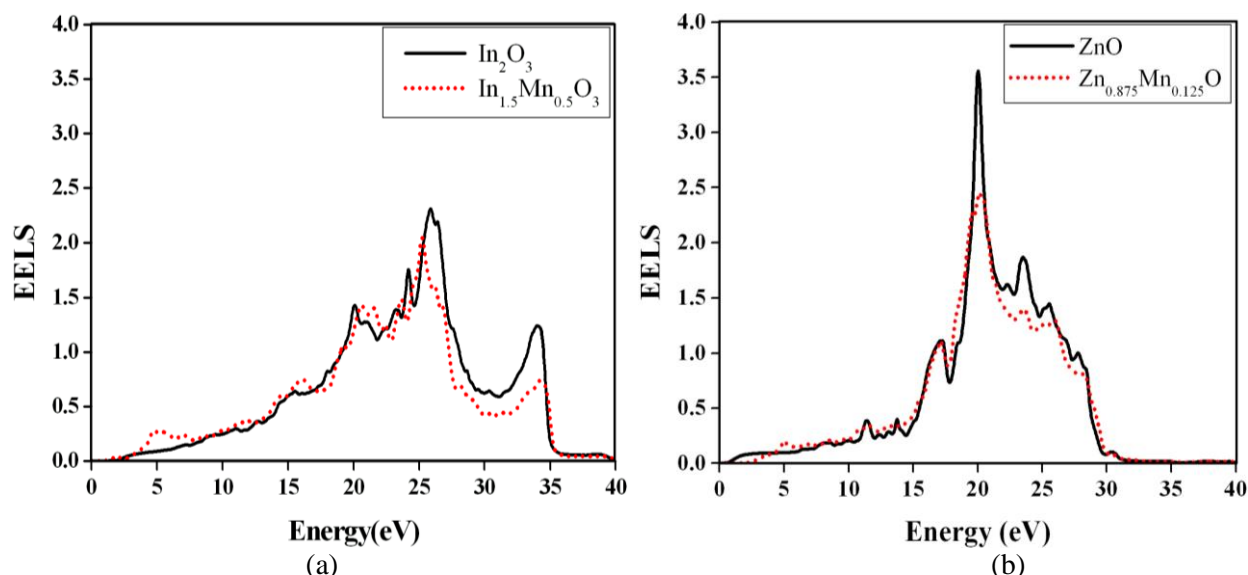(a)   (b)

Fig. 6. Electron energy loss for: (a) In_2O_3 and $In_{1.5}Mn_{0.5}O_3$ (b) ZnO and $Zn_{0.875}Mn_{0.125}O$

Table 3. Calculated plasmon energy for In_2O_3 and ZnO in pure and alloyed with Mn

Compound	$h\omega_P$ (eV)
In_2O_3	25.81
$In_{1.5}Mn_{0.5}O_3$	25.18
ZnO	20.01
$Zn_{0.875}Mn_{0.125}O$	20.19

CONCLUSION

In the present study, the structural and optical properties of In_2O_3 and ZnO in undoped and doped with Mn states are investigated by utilizing the full potential-linearized augmented plane wave (FP-LAPW) method with the generalized gradient approximation (GGA). The obtained results indicate that In_2O_3 and ZnO energy gap is changed by substituting Mn element on In, Zn in In_2O_3 and ZnO, respectively. Doping In_2O_3 with Mn brings about a decrease in the band gap while it increases for doped ZnO.

Calculating the optical spectra have been carried out in the energy range 0–40 eV. The obtained high-frequency dielectric constant $\varepsilon(\infty)$ shows that refraction index for In_2O_3 is increased by adding Mn, $\varepsilon(\infty)$ whereas this value is decreased for ZnO compound.

REFERENCES

1. C.H. Ahn, J.M. Triscone, J. Mannhart, *Nature.* **424**, 1015 (2003).
2. F. Amiri, F. Foroutan, M.M. Amiri, H.A. Rahnamaye, *Ind. J. Science Technol.*, **10**, 1 (2017).
3. D.S.Ginley, M.P. Taylor, M.F.A.M. van Hest, D. Young, C.W. Teplin, J.L. Alleman, M.S. Dabney, P. Parilla, L.M. Gedvilas, B.M. Keyes, ,B. To, D. Readey, J.D. Perkins, Combinatorial exploration of novel transparent conducting oxide materials. *National Renewable Energy Laboratory, Colorado,* 7-10(*2005).*
4. S. Laux, N. Kaiser, A. Zöller, R. Götzelmann, H. Lauth H. Bernitzki, *Thin Solid Films*, **335**, 1 (1998).
5. H.A. Rahnamaye Aliabad, S.M. Hosseini, A. Kompany, A. Youssefi, E. Attaran Kakhki, *Phys. Status Solidi B*. January, **246**, 1072 (2009).
6. S.Zh. Karazhanov, P. Ravindran, P. Vajeeston, A. Ulyashin, T.G. Finstad, H. Fjellvag, *Phys. Rev. B*. **76**, 075129 (2007).
7. A. Walsh, L.F. Juarez, D. Silva, S.H. Wei, C. Körber, A. Klein et al., *Phys. Rev. Lett*. Apr, **100**, 167402 (2008).
8. Ü. Özgür, Y.I. Alivov, C. Liu, A. Teke, M.A. Reshchikov, S. Doğan et al. *J. Appl. Phys.,* **98**, 041301 (2005).
9. H. Morkoç, Ü. Özgür, Zinc Oxide Fundamentals, Materials and Device Technology. WILEY-VCH Publication Company: Weinheim-Deutsche, (2009).
10. M. Petersen, F. Wagner, L. Hufnagel, M. Scheffler, P. Blaha, K. Schwarz, *Comp. Phys. Commun*, **126**, 294 (2000).
11. J.P. Perdew, J.A. Chevary, S.H. Vosko, K.A. Jackson M.R. Pederson, D.J. Singh et al., *Phys. Rev. B*. Sep, **46**, 6671 (1992).
12. P. Blaha, K. Schwarz, G. Madsen, D. Kvasnicka, J. Luitz, Institute for Materials Chemistry. TU Vienna (http://www.wien2k.at/).
13. A. Belsky, M. Hellenbrandt, V.L. Karen, P. Luksch, *Acta Cryst. B*, **58**, 364 (2002).

14. A. Zaoui, M. Ferhat, R. Ahuja, *Appl. Phys. Lett*. **94**, 102102 (2009).

15. I. Hamberg, C.G. Granqvist, K.F. Berggren, B.E. Sernelius, L. Engstrom, *Phys. Rev. B*. **30**, 3240 (1984).

16. H.G. Swamy, P.J. Reddy, *Semicond. Sci. Technol*, **5**, 980 (1990).

17. K. Palandage, G.W. Fernando, *Phys. Lett. A*., **374**, 2879 (2010).

18. Zhu YZ, Chen GD, Ye H, A. Walsh, C.Y. Moon, S.H. Wei, *Phys Rev. B*. June, **77**, 245209 (2008).

19. F. Fuchs, F. Bechstedt, *Phys. Rev. B*. Apr, **77**, 155107 (2008).

20. P. Pratap, Y.P.V. Subbaiah, M. Devika, K.T.R. Reddy *Mater. Chem. Phys*, **100**, 375 (2006).

21. H. Yoshikawa, S. Adachi *Jpn. J. Appl. Phys*, **36**, 6237 (1997).

22. S. Loughin, R.H. French, L.K. Noyer, Ching WY, Xu YN,. *J. Phys. D*., **29**, 1740 (1996).

23. C. Ambrosch-Draxl, J.O. Sofo, *Computer Phys. Commun*. July, **175**, 1 (2006).